Electric Power Systems Research 248 (2025) 111890

Contents lists available at ScienceDirect

Electric Power Systems Research

journal homepage: www.elsevier.com/locate/epsr

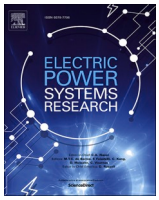

A pattern recognition based tool for smart distribution networks reconfiguration

Andrea Bonfiglio *, Alice La Fata, Manuela Minetti

University of Genoa, Department of Electrical, Electronic, Telecommunications Engineering and Naval Architecture, Genoa Italy

ARTICLE INFO

Keywords:
Energy transition
Renewable energy sources integration
Distribution grids
Pattern recognition

ABSTRACT

In power distribution networks, the growing integration of Renewable Energy Sources (RES) is increasing operational issues related to undesirable steady-state working conditions. In this context, this paper proposes a novel approach of distribution power system management, referred to as Smart Distribution Area Control Architecture (SDACA), based on a pattern recognition algorithm, that allows exploiting network reconfiguration contactors to find the most suitable grid configuration to mitigate steady-state network violations due to relevant share of RES hosted by the grid. The SDACA leverages real-time data acquisition and forecasted power generation and consumption data to determine the optimal switch states, enhancing the operational reliability and efficiency of the distribution network. To estimate the optimal network configuration, a pattern recognition model is implemented. Specifically, the extreme gradient boosting algorithm is used, exploiting its fast-training procedure and the rapid execution time. The performance of the proposed SDACA tool is validated in a realistic distribution grid layout, exhibiting up to 90 % accuracy in the identification of the network configuration, a capability of reducing the number of voltage violations of roughly 65 % in the considered test case network, and a 99 % effectiveness in minimizing voltage violations compared to the maximum achievable impact of optimal feeder reconfiguration on voltage violations.

1. Introduction

The increasing number of Renewable Energy Sources (RES) has introduced multiple challenges for power grids for both the transmission and distribution systems. On the one hand, for transmission networks, the increasing share of RES is leading to the reduction of traditional synchronous generators based power plants connected to the grid, with consequent issues on the system inertia, primary regulating energy and short-circuit capacity, leading to possible negative effects on frequency and voltage stability [1,2]. Distribution grids, on the other hand, are the areas of the electricity system where the largest share of RES is actually installed, and this is causing serious problems with power quality aspects such as voltage profiles [3,4], line congestions and primary substation transformer overloading [2]. As generally known, novel flexibility services are essential to make the power grid capable of enduring and actuating the upcoming energy transition. As far as distribution systems are concerned, several flexibility services have been studied on the end user side. As an example, Microgrids (MGs) have been often studied as a suitable framework to provide grid support services, as instance by including in grid connected MG controllers and energy management systems, suitable reactive power control strategies to support grid voltages [5,6]. Additionally, the possibility of MGs intentional islanding to alleviate the distribution grid from possible fluctuation or RES has been addressed by recent research works [7–10]. In this context, the Distribution System Operators (DSOs) is also interested in introducing novel power grid management strategies to improve grid flexibility and resiliency. On this subject, network reconfiguration is a relevant and promising feature to be considered. Usually, distribution grids are designed to have several ring reclosure for well-known security/redundancy availability of power supply, but these networks are often operated in radial condition for a much easier management of power flows and system protection [11]. However, the possibility of dynamically reconfiguring the network switching from a radial configuration to a weakly meshed one is a solution that DSOs may apply to mitigate steady state violation of power grids with relevant share of RES. To this end, DSOs require advanced tools and methodologies to identify the optimal topology of the distribution network to cope with specific operational scenarios. Within this framework, the process of Feeder Reconfiguration (FRC) implemented by the DSO is automated by utilizing real-time operation and control methods. Thanks to these, the radial topology of the distribution network may change depending on

* Corresponding author.
E-mail address: a.bonfiglio@unige.it (A. Bonfiglio).

https://doi.org/10.1016/j.epsr.2025.111890
Received 21 January 2025; Received in revised form 26 May 2025; Accepted 27 May 2025
Available online 5 June 2025

Nomenclature

Classification and Regression Trees CART
Distribution System Operator DSO
eXtreme Gradient Boosting XGB
Feeder Reconfiguration FRC
Microgrids MG
Neural Network NN
Pattern Recognition PR
Photovoltaic PV
Renewable Energy Sources RES
Smart Distribution Area Control Architecture SDACA
Wind Turbines WT

the opening or closing positions of the involved switches [12]. Specifically, the ability to reconfigure the involved feeders enables the distribution system to operate both reliably and economically, since it may allow a reduction in power loss and in components overloading, an improvement in voltage profile, increased voltage stability and balancing of the involved loads [13]. However, the discrete nature of the switches introduces complexity in applying traditional optimization methods to the multi-objective FRC problem. Precisely, in terms of optimization, network reconfiguration is a mixed-binary nonlinear optimization problem where binary variables represent the switch states and continuous variables model the involved electrical quantities. Although the globally optimal configuration can theoretically be obtained by enumerating all feasible configurations and choosing the one that maximizes the problem objective, the process becomes impractical even for moderate size networks since execution time scales exponentially with the number of nodes and switches [14]. Specifically, the intrinsic computational complexity of the combinatorial optimization problem may drive to prohibitive computational time when dealing with largescale distribution systems with many buses and switches [15]. Additionally, the optimization of these problems requires knowledge of the stochastic processes used to model the uncertain parameters, which are often not readily available in practice. To simplify such problem, traditional methods propose to convert the multi-objective optimization problem to a single objective optimization one [12] and, typically, the reconfiguration problem is modelled as a combinatorial problem with a complex space due to current and voltage constraints. Under this perspective, in the last decades, several procedures have been proposed as solutions. By way of example, the heuristic approach was used in [16]; however, the drawback of this approach is the need for local search methods that may lead to suboptimal results due to sensitivity to initial conditions. Additionally, deterministic methods have also been explored in the last years thanks to the advances in the computational capabilities [14,17–19]. Nevertheless, two main limitations persist: piecewise linear approximations may result in unrealistic modelling and can increase the computational burden [20,21], and incomplete network parameters can lead physical model-based methods to sub-optimal solutions [22]. To address the issue, stochastic optimization algorithms have also been proposed [23–25]. Though, as the network expands and the number of possible solutions increase, the convergence rate tends to slow down, and, in some cases, it may fail to achieve optimal convergence results. Trying to overcome these limitations, in the recent years, some research works related to the field have started introducing Pattern Recognition (PR) models, with the goal of mapping the extremely non-linear relationship between the load/generation and the system topologies required for the FRC [26]. As an example, in [27–30] Neural Networks (NNs) were used to determine the system topology that reduces the power losses according to the variation of load patterns. However, the complexity of the NNs in [27–30] prompts an extremely high number of parameters to be learnt, thus requiring a huge training dataset that could result in limiting the adaptability of the tool to different network topologies [31]. Under this perspective, recently, the study conducted by the authors of [15] to estimate the operational state of the system - classified into three predefined categories, i.e., normal state, intermediate state, and emergency state - highlighted that decision tree-based methods offer significantly faster computation compared to other PR models. Furthermore, even though, generally, decision tree-based methods, may have difficulties to effectively generalize data patterns, results obtained in [15] show higher accuracies with respect, as instance, to the ones obtained in [27].

For a better understanding of the current state-of-the-art and the limitations of the described solutions, a brief summary is proposed in Table 1.

Within this state-of-the-art, this paper proposes an effective Smart Distribution Area Control Architecture (SDACA) for DSOs, based on a PR algorithm, to determine the optimal network configuration that minimizes *i)* overvoltage and undervoltage issues at the nodes of the distribution network, and *ii)* the number of switches reclosures, while ensuring rapid response times. The proposed PR approach aims at exploiting the chance of obtaining a rapid response to contemporaneously achieve the possibility of planning network configuration based on power profile estimations, and the possibility of detecting possible dangerous situations. Precisely, SDACA is designed to receive input data referred to the power produced and consumed by the technologies involved in a generic radial network. The output is the optimal switches' states that allows to determine the network topology to be implemented to minimize overvoltage and undervoltage issues at the network nodes, as well as the number of reclosures. Within SDACA, a PR algorithm is implemented to evaluate the network configurations. For the specific application, the eXtreme Gradient Boosting (XGB) algorithm, i.e., a PR algorithm that is part of the ensemble learning of tree-based methods, is used, leveraging its valuable skills in many engineering fields [32,33], such as the fast-training procedure and the rapid execution time. These characteristics allows to easily adapt the proposed tool to different multiple bus distribution networks and to estimate the FRC of all alternative network topologies in a short time intervals, thus making it suitable for large distribution grid applications. The effectiveness of the SDACA is evaluated on the IEEE 33-node network, considering the reclosures presented in [34]. The results are compared in terms of voltage violations with the configuration in which the distribution network is operated the radial configuration. To sum up, the novelty of the proposed research work are: *(i)* the implementation of an extremely flexible procedure to map the distribution network topology along with system parameters based on a PR model able to easily adapt to the network topology, *(ii)* the possibility to estimate the best network configuration among all alternatives, to determine the optimal one that minimizes under(over)voltage issues and the number of switches reclosures, in a short time interval thanks to the fast execution time of the PR model implemented. This feature avoids the need of implementing nonlinear optimization problems, whose execution time may

Table 1
State-of-the-Art in the FRC problems field.

Approach	References	Limitation
Heuristic method	[16]	Suboptimal results, sensitivity to initial conditions.
Deterministic Optimization Methods	[14,17–19]	High computational burden, dependence on precise network parameters, scalability issues.
Stochastic Optimization	[23–25]	High computational burden, possible convergence issues.
Neural Network	[27–30]	Need for large datasets to set the network parameters.
K-Nearest Neighbor	[15]	Sensitive to the setting of the number of neighbours.
Decision Trees	[15]	Difficulty to effectively generalize (tendency to overfitting).

exponentially increase with the number of nodes and switches.

The paper is organized as follows. Section 2 proposes an overview of the methodology implemented, Section 3 details the case study used to test the proposed approach, and Section 4 discusses the related results. Finally, Section 5 provides some conclusive remarks and future developments.

2. Methodology

SDACA is designed to support DSOs in managing distribution power system where grid FRC is possible and allows to schedule the most efficient action on the grid based on historical data, actual measurement and forecasts. A generic portion of a distribution network is considered. The considered network operates under normal conditions in a radial configuration and is characterized by N_S switches that allows weakly meshing the grid. By evaluating all possible combinations of switch states, up to 2^{N_S} network configurations can be identified. Supposing that the share of RES in this grid is sufficiently high, the grid operating in the radial configuration may experience over or under voltage issues, that may be solved or alleviated in one of the 2^{N_S} alternative configurations. To this end, the SDACA tool is designed to analyse the expected generation and load behaviours to provide a definition of the most suitable grid configuration among the available ones. To this goal, a PR algorithm is designed and implemented in SDACA. The necessary step to implement and use SDACA can be summarised as follows:

i. Network Definition: the area of the distribution network to be managed by the SDACA needs to be identified characterizing the number grid configurations associated to the switch state and categorized grid status according to over- or under-voltage conditions;
ii. Scoring definition: a scoring system is defined matching the different grid configurations with grid status characterized by overvoltage and undervoltage issues;
iii. Dataset Generation: a Power Profile Dataset is used to run load flow calculations to assess the voltage values at the network nodes and the various configuration of the network, and to score each load flow calculation with the scoring defined at the previous step. At the end of this step, an Output Dataset is generated by the integration of the Power Profile Dataset with the scoring for each network configuration;
iv. Algorithm implementation: a random portion of the Output Dataset is used to as training set for the training phase of the PR algorithm. The remaining portion of the Output Dataset is used to test the algorithm. The target of the algorithm is to estimate the score associated to each combination of grid configuration and grid status, as defined by the scoring system of step ii. The training set is used to identify the most suitable algorithm parameters, while the test set is used to validate the effectiveness of the algorithm itself.
v. Optimal configuration definition: SDACA is fed with a grid expected working condition, i.e., active and reactive power for each node, and outputs the configuration (switch states) providing the best expected score, thus suggesting the corresponding grid configuration for the considered working point.

The methodological workflow of the SDACA implementation is sketched in Fig. 1.

2.1. Network definition

The SDACA tool is designed for a distribution network operating under normal conditions in a radial configuration. The distribution network consists of N nodes, N_L lines, and N_S switches. Considering all possible combinations of the switches states, up to 2^{N_S} network configurations can be identified. The considered area of the network includes the primary transformer substation and the medium-voltage distribution network downstream of the transformer. Each line is characterized by the related resistance and reactance values. The network may include N_{MG} Microgrids (MGs), N_{PV} Photovoltaic (PV) systems, N_{WT} Wind Turbines (WTs), and N_{Load} loads. By knowing active and reactive power associated to each of the previously mentioned technologies (assuming the high voltage side of the primary substation transformer as slack bus) one can assess voltage profiles for every time frame considered. With this results, one can evaluate overvoltage and undervoltage condition with respect maximum and minimum voltage levels, v_{max} and v_{max}. Specifically, to reduce the number of information to be used in the definition of the algorithm, nodes are grouped in N_c clusters and voltage violation shall be associated to the defined clusters. For sake of clarity, it is highlighted that clusters should be defined by grouping adjacent nodes with similar voltage behaviour, this way it will be uncommon to encounter nodes with both overvoltages and undervoltages within the same cluster simultaneously.

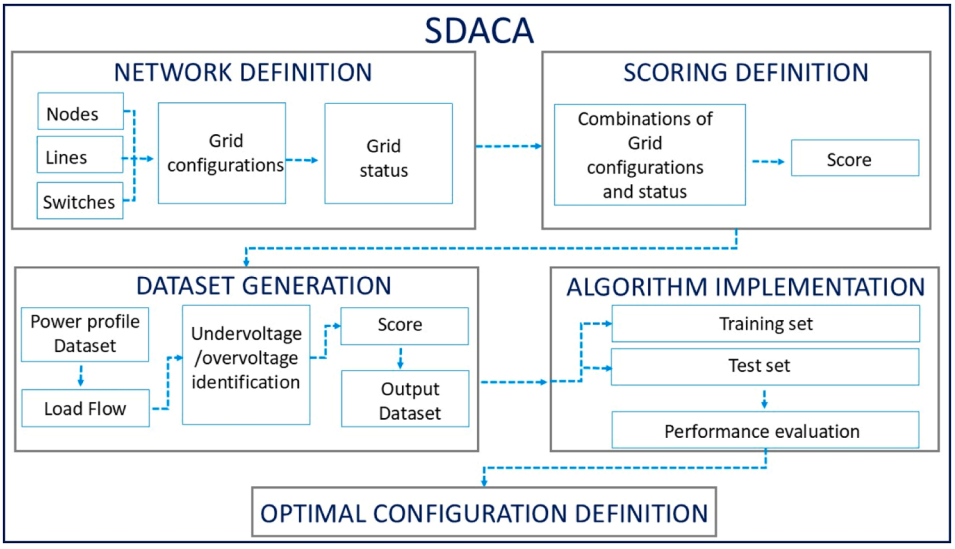

Fig. 1. Flowchart of the methodology used to implement SDACA.

2.2. Scoring system definition

A scoring system needs to be defined to select the priority of the desired network working condition. More specifically, from the one hand, the network 2^{N_S} alternative configurations are considered according to all possible combinations of switch states, where the radial one is the most wanted, followed by configurations with the smaller number of meshes, i.e., lower number of closed switches. These configurations are labelled respectively as Radial, Configuration 1, … , Configuration $2^{N_S}-1$.

Cluster over- and under-voltage violations are classified corresponding, respectively, to no cluster with under or over voltage violation (ideal condition), one cluster with voltage violation, two clusters with voltage violations and so on until, N_c clusters experience voltage violations. Hence, the scoring system considers N_c+1 clusters conditions. In the following, these conditions shall be referred to as V_0 if no cluster shows voltage violations, V_1 if at least one cluster shows voltage violations, and so on until condition V_{Nc} , corresponding to the condition where all clusters show voltage violations.

This results in a total number of scores to be defined equal to $2^{N_S}\cdot(N_c+1)$.

The scoring procedure can be then generalized as follows. Let us define the maximum score, S_{max}, as:

$$S_{\max} = 2^{N_s}\cdot(N_c+1) \tag{1}$$

The maximum score is associated to the most wanted condition, i.e., the radial one without any voltage violation. Score reduction may firstly consider the condition with no violation but progressive increasing of closed switches; hence, after considering all configurations matched with condition V_0, the progressive scoring decreasing shall pass class V_1 starting back from the radial configuration and then passing at the other configuration. This procedure shall be followed until covering all possibilities getting to the lowest score that shall correspond to one.

An effective way to represent the scoring system is by organizing it in a configuration - violation matrix, as the one reported in Table 2. Moving from up to down, and from left to right the conditions get worse and so does the scoring.

2.3. Dataset generation

As abovementioned, initially, Power Profile Dataset is created. This dataset is used to run load flow calculations and to compute the voltage values at the network nodes. Subsequently, the scoring system allows to associate a score to each grid configuration linked with the related grid status. Thereafter, the Power Profile Dataset is merged with the scores defined and the Output Dataset is created. The Output Dataset represents the input of the algorithm, i.e., the so-called feature vector. A portion of the feature vector is fed to the algorithm to allow the training phase. Specifically, the feature vector includes, for all the technologies involved, the profile of N_t elements, i.e., the profiles of active powers provided by the N_{PV} PV plants and by the N_{WT} WT systems, the profiles of active powers consumed by the N_{Load} loads, and the profiles of active power exchanged with the grid by the N_{MG} MGs. Moreover, the status of all the N_S switches, specified by a value that allows to differentiate the open and the closed status, is included within the feature vector. Thereafter, the scores associated by the scoring system to the possible combinations of the switches and clusters configurations are included within the feature vector. The values associated with these scores represent the target of the algorithm, i.e., the output the algorithm is trained to estimate. For consistency with the terminology used for the implementation of the algorithm, from now on, these scores will be referred to as classes.

Table 2
Scoring Matrix definition.

	$\mathbf{V_0}$	$\mathbf{V_1}$	$\mathbf{V_2}$	…	$\boldsymbol{V_{N_c}}$
Radial	S_{max}	$S_{max}-2^{N_S}$	$S_{max}-2\cdot2^{N_S}$	…	$S_{max}-N_c\cdot2^{N_S}$
Configuration 1	$S_{max}-1$	$S_{max}-2^{N_S}-1$	$S_{max}-2\cdot2^{N_S}-1$	…	$S_{max}-N_c\cdot2^{N_S}-1$
…..	…	…	…	…	…
…..	…	…	…	…	…
Configuration 2^{N_S}-1	$S_{max}-2^{N_S}+1$	$S_{max}-2\cdot2^{N_S}+1$	$S_{max}-3\cdot2^{N_S}+1$	…	*1*

2.4. Algorithm implementation

The algorithm implemented within SDACA is a PR algorithm. Precisely, considering the demonstrated abilities in various engineering fields [35,36], the selected algorithm is the XGB. The motivation for implementing a PR algorithm has been driven by the demonstrated abilities in dealing with large datasets because of the tree-based architecture that, compared to NNs' one, require less training time. In addition, the architecture of XGB algorithms allows to capture complex patterns and dependencies among the features without the need of computationally intensive time to map the relationship among the inputs and the target [37]. This characteristic allows tree-based models to consistently outperform standard deep models on tabular-style datasets, where features are individually meaningful [32].

Moreover, the application of PR algorithm to learn the relationship between network topology and the best configuration from historical data allows to overcome scalability issues typical of methodologies to solve the FRC problem based on optimization algorithms. Indeed, as highlighted in [15], when dealing with FRC problems, these issues are due to the computational time required to seek the best solution (if feasible) and to the fact that the optimization of these problems requires knowledge of the stochastic processes of the uncertain parameters, which are often unknown. From this perspective, the recent application of PR algorithms to solve FRC problems turned out to effectively and rapidly evaluate the network reconfiguration based on actual contingencies including the possibility of easily adapt the model to larger and more complex distribution networks.

Under this perspective, it should be noted that XGB classification algorithms are generally scalable and well-suited for large datasets, thanks to their parallelized tree boosting structure [38]. In this context, potential challenges may include increased computational time required for the training phase with a growing number of classes, and the need for careful hyperparameter tuning to avoid overfitting or underperformance. Nevertheless, the computational time to output the estimated class (score) of unseen samples can be controlled by properly setting the features by tree parameter, as detailed in [38].

For the specific application, the XGB algorithm is used as a classification algorithm to estimate the class (score) assigned to each combination of switches states and clusters configurations.

In the following, the basic principles of the XGB algorithm are recalled. From now on bold lower-case letters indicate vectors, and non-bold letters denote scalars.

The XGB algorithm is part of the Classification and Regression Trees (CART) models, also named decision trees. Precisely, CART models are defined by recursively partitioning the input space and defining a local model in each resulting region of input space [38]. More in detail, CART models can be represented by a tree, with one leaf per region. For regression tasks, the overall result is that the input space is partitioned into regions and a mean response is associated with each region. For classification problems, the leaves contain a distribution over the class labels, rather than just the mean response. Hence, for classification purposes, the output space is a set of N_{class} unordered and mutually exclusive labels, referred to as classes. The main limitation of traditional CART models lies in the difficulty to effectively generalize, often resulting in overfitting to the training data and reduced performance when applied to unseen datasets [38]. To reduce the intrinsic variance of

decision trees, a procedure referred to as ensemble learning allows building a prediction model by combining the strengths of a collection of simpler base models Precisely, ensemble learning is a technique in which multiple models (often referred to as base models or weak learners) are combined to produce a stronger model that performs better than any individual model. Specifically, for a given dataset $D = \{(\boldsymbol{x}_1, y_1), \ldots, (\boldsymbol{x}_n, y_n)\}$ composed of n samples, let $\boldsymbol{x}_\ell$ be the feature vector and y_ℓ the real value assumed by the target referred to the ℓ-th sample. The task of the model is to learn a mapping function f from the inputs, collected in the feature vector $\boldsymbol{x}$, to outputs, collected in the vector $\boldsymbol{y}$. An ensemble learning model has the form:

$$f(\boldsymbol{y}|\boldsymbol{x};\boldsymbol{\theta}) = \frac{1}{|M|}\sum_{m\in M} f_m(\boldsymbol{y}|\boldsymbol{x};\boldsymbol{\theta}_m) \tag{2}$$

where f_m is the m -th base model, M is the total number of base models, $\boldsymbol{\theta}_m$ is a set of parameters defining the model. The predictions of the base models are aggregated in different ways (e.g., averaging, majority voting) to make the final decision. Several methods can be used to make the final decision, such as stacking, bagging, random forests, boosting. Independently on the method to estimate the output, the goal of the algorithm is to minimize the empirical loss, i.e., the difference between the actual value y_ℓ and the predicted value $\hat{y}_\ell$. Thus, let *Loss* denote a generic differentiable loss function, measuring the difference between y_ℓ and $\hat{y}_\ell$, the empirical loss can be defined as:

$$Loss(f) = \sum_{\ell=1}^{n} Loss(y_\ell, \hat{y}_\ell) \tag{3}$$

Among ensemble learning models, gradient boosting techniques are implemented to solve a model of the form (2) by performing gradient descent in the space of functions [38]. Precisely, boosting is an algorithm for sequentially fitting additive models where each F_m model is a binary classifier that returns $F_m \in \{-1, +1\}$. Among tree bosting techniques, XGB is a very efficient and widely used implementation of gradient boosted trees [38]. Specifically, it adds a regularizer on the tree complexity and it samples features at internal nodes. In more detail, XGB aims at minimizing the sum of the loss function and the regularization term, defined as:

$$Loss(f) = \sum_{\ell=1}^{n} Loss(y_\ell, \hat{y}_\ell) + \sum_{m=1}^{M} \Omega(f_m) \tag{4}$$

$$\Omega(f_m) = \alpha J + \frac{1}{2}\beta\sum_{j=1}^{J}\omega_j^2 \tag{5}$$

where $\Omega(f_m)$ represents the regularization term referred to the identified mapping function from the inputs $(\boldsymbol{x}_\ell)$ to the targets (y_ℓ) used to control the model complexity, and J, ω_j, α, and β are parameters defining the model. Hence, for the m-th tree, referred to as the F_m model, the loss is given by:

$$Loss_m(F_m) = \sum_{\ell=1}^{n} Loss(y_\ell, f_{m-1}(\boldsymbol{x}_i;\boldsymbol{\theta}_{m-1}) + F_m(\boldsymbol{x}_\ell;\boldsymbol{\theta}_m) + \Omega(F_m(\boldsymbol{x}_\ell;\boldsymbol{\theta}_m))) + const \tag{6}$$

Considering the wide application in many engineering fields [38], the selected loss function to be minimized is the softmax function, i.e., a function that takes the vector of scores and converts them into probabilities values between 0 and 1, so that the sum of the probability referred to each score (class) equals 1.

The optimized parameters in the model are chosen because of the results obtained in previous works in the field [36,39]. Specifically, the maximum depth of decision trees, the features by tree, the number of estimators and the learning rate are optimized since outcomes of [39,40] revealed their influence in the estimation skills of the model.

Finally, it is worth recalling that PR algorithms are based on the idea to train and test the model on different sets of data. Specifically, the training set, i.e., a subset of the available data within the Output Dataset, is used to train the model by allowing it to learn patterns, relationships, and structures within the data during the so-called training phase. At the end of the training phase, the test phase is performed to evaluate the model performance on unseen data. Hence, the test set, containing data not used for the training phase, is used to perform the test phase, devoted to the computation of the evaluation metrics. To train the algorithm, the intervals in which the model parameters are sought are defined and, within the training phase, the optimal one for each set is selected to reach the best performance. Following, the algorithm is tested by providing only the power profiles and switches state to the tool which will output an estimation of the score. Hence, the predicted score is compared to the score obtained by load flow calculation done when the Output Dataset was created so that one can assess the performance of the algorithm prediction. It is worth pointing out that this phase is used only to assess if the PR algorithm is able to correctly predict to scoring of the analysed sample, thus providing an evaluation of its effectiveness.

2.5. Optimal configuration definition

This last part of the methodology is the actual utilization of the tool defined until now. Once the algorithm has been trained and tested, it can be used to support the choice of the suitable network configuration. The SDACA tool in this phase is fed with expected or measured active and reactive power of the grid busses, using the same structure of the Power Profile Dataset. The algorithm then provides an evaluation of the working point and outputs the score prediction for all possible network configuration. Hence, the one characterized by the higher score is identified as the optimal network configuration for the considered working condition.

3. Case study definition

3.1. Distribution network characterization and analysis

For sake of demonstration, the tool was developed for a 33-node benchmark distribution network [34] depicted in Fig. 2; however, as discussed in the previous section, the methodology is easily scalable to larger networks with a higher number of nodes and possible meshed configurations without any loss of generality. The test-case distribution network consists of $N = 33$ nodes with $N_L = 32$ connection lines that can be integrated in the radial distribution network through the management of the N_S =3 switches, namely INT_{13-33}, INT_{18-25}, and INT_{5-22}, as shown in Fig. 2. The network topology and its possible reconfigurations are detailed in [34]. Specifically, considering all combinations of switch states, there are $2^{N_S} = 2^3$, i.e., eight possible configurations of the network. Precisely, associating a value equal to one (zero) to indicate that the switch is open (closed), the mapping of the eight grid configurations is reported in Table 3.

The resistances and reactances of the recloser lines are considered negligible for the purposes of this analysis. Nodes are organized into four clusters, referred to as $Cluster_{1-22}$, $Cluster_{26-33}$, $Cluster_{7-18}$, $Cluster_{4-25}$, as detailed in Table 4.

The distribution network operates at a voltage level of 12.66 kV, while the transmission network operates at 132 kV. The primary substation transformer has a rated apparent power of 18 MVA with a 132 kV/12.66 kV voltage ratio, 8 % short-circuit voltage, and an R/X ratio of 1/10. The parameters of the distribution network lines, including resistance, referred to as $r_{l,ik}$ (where l indicates the line between the node i and k), and reactance, referred to as $x_{l,ik}$, are detailed in [34] and reported in the attached dataset[1]. Each node in the network is connected to one of the following technologies: PV, WT, Load or MG. The nodes and their associated technologies and power rating are listed in Table 5. To test the methodology proposed, suitable profiles need to be available for

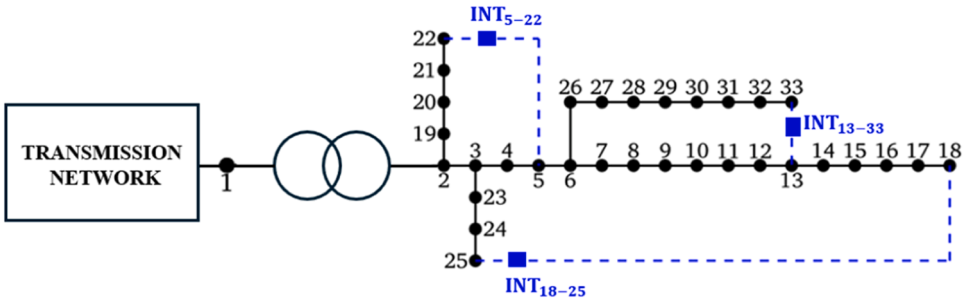

Fig. 2. 33-node distribution network.

Table 3
Grid configuration definition according to switch status.

Configuration	Switches status	Configuration	Switches status
Radial	INT_{13-33} +INT_{18-25} +INT_{5-22} =3	Configuration 4	INT_{5-22} =1
Configuration 1	INT_{18-25} +INT_{5-22} =2	Configuration 5	INT_{18-25} =1
Configuration 2	INT_{13-33} +INT_{5-22} =2	Configuration 6	INT_{13-33} =1
Configuration 3	INT_{13-33} +INT_{18-25} =2	Configuration 7	INT_{13-33} +INT_{18-25} +INT_{5-22} =0

Table 4
Clusters definition.

Group	Nodes	Group	Nodes
$Cluster_{1-22}$	1, 2, 3, 19, 20, 21, 22	$Cluster_{7-18}$	7, 8, 9, 10, 11, 12, 13, 14, 15, 16, 17, 18
$Cluster_{26-33}$	26, 27, 28, 29, 30, 31, 32, 33	$Cluster_{4-25}$	4, 5, 6, 23, 24, 25

each technology in the grid. For this purpose, hourly sampled profiles for the PV, WT and loads have been retrieved from the Italian DSO database and thus they are referred to a realistic scenario located in North Italy.[1] From this source, sets of four weeks have been extracted, representative for each season of the year for 11 years. In detail, the first week of January, April, August, and October are considered for the years from 2011 to 2022. These profiles have been normalized and scaled according to the technologies power rating at each node reported in Table 5.

It is worth pointing out that the grid has been characterized by a relevant amount of RES to create voltage issue and to show how the SDACA tool can contribute to improving power distribution grid capacity to host RES. For a more realistic and accurate characterization of the grid, reactive power supplied by RES is defined according to the Voltage vs. Reactive Power curve represented in Fig. 3, as prescribed by the Italian distribution system grid code requirements CEI 0–16 [41]. For loads and MG power factor has been assumed equal to 0.9 lagging.

As a result, 672 working points are considered for each year, resulting in a total of 7392 working points. To perform all load flow calculations, node 1 is defined as the slack imposing voltage equal to 1 pu. and zero phase angle. The remaining nodes are considered as PQ nodes, with assigned active and reactive power values based on the profiles included in the Power Profile Dataset.

75 % data taken from the Power Profile Dataset, corresponding to 44,352 samples, is used to train the algorithm generating the training portion of the Output Dataset, while the remaining 25 % corresponding to 14,784 samples, is used to create the first portion of the Output Dataset used for the test phase, namely Test Set 1.

[1] The Power Profile Dataset is attached to the submission material. The provided profiles are normalized according to the size of the related technology.

Moreover, a sensitivity analysis to evaluate the performance of the proposed SDACA tool under input parameters variation is performed generating two additional test sets. To this goal, inputs (features) that can experience stochastic variations have been perturbed following a widely applied procedure [42]. Precisely, inputs that can experience stochastic variations in the extracted 25 % of the Power Profile Dataset, e.g. RES production and loads, have all been perturbed of random values uniformly distributed over predefined intervals. A ± 5 % interval is considered to generate the so referred Test Set 2, and a ± 10 % interval is considered for the Test Set 3.

3.2. Scoring system definition for the case study

Considering the possible 2^{N_S} combinations of switch states referred to the working points in the Power Profile Dataset, load flow calculations are performed for 2^{N_S}·7,392 elements, from now on referred to as samples. To define the scoring system that allows to associate a score (class) to each sample, the values referring to the N_c=4 clusters conditions are used. More in details, the value associated to each cluster is set to positive one if the cluster contains at least one node experiencing overvoltage, to negative one if at least one node exhibit undervoltage, and to 0 if all node voltages are within the 0.95 pu. - 1.05 pu. range, representing, respectively, v_{max} and v_{max}. According to the analysis detailed in Section 2.2, in presence of four clusters, five conditions are possible, as detailed in Table 6. Under these assumptions, 40 combinations among the switches status (Table 3) and the clusters condition (Table 6) are identified and differentiated. To each of them, the scoring system assigns a value, corresponding to the class in which the configuration is classified. Precisely, according to (1), the scoring system is defined by initially assigning a value of S_{max}=40 to the best condition of the considered network, corresponding to the radial configuration in which no clusters experiences under(over)voltages and proceeding as detailed in Section 2.2. The resulting scoring matrix is reported in Table 7. At the end of the association of the scores to each cluster condition and switches configuration, the Power Profile Dataset is merged with the scores associated and Output Dataset is created. Output Dataset is thus composed of 2^3·7,392 samples.

3.3. Algorithm implementation for the considered case study

To train the model, the XGB algorithm receives as input the training portion of the Output Dataset. Denoting with C_ℓ the real class(score) associated to the ℓ-th sample (following the formulation in Table 7), the goal of the model is to estimate such class. The estimate corresponds to the class reaching the highest probability and is referred to as $\widehat{C}_\ell$. By way of example, Table 8 shows two samples extracted from the training portion of the Output Dataset. For the sake of compactness, in Table 8 only some values referred to the PV, WT and load profiles are reported. Moreover, in Table 8, for each technology, the N_e elements are identified by the related subscript, e.g., PV_1 refers to the first involved PV plant.

Additionally, the sets referred to the parameters to be optimized are chosen because of the results obtained in previous works in the field [36,

Table 5
Type and rated power of the 33-Node Bus System technologies.

Node	Type	Size [MVA]	Node	Type	Size [MVA]	Node	Type	Size [MVA]
1	–	–	12	Load	1.00	23	PV	3.25
2	–	–	13	WT	1.00	24	Load	0.40
3	PV	3.75	14	Load	0.50	25	WT	2.50
4	Load	0.50	15	MG	2.00	26	Load	0.50
5	WT	2.50	16	PV	1.75	27	WT	3.00
6	Load	0.25	17	Load	0.50	28	PV	1.50
7	Load	0.40	18	Load	0.50	29	Load	0.25
8	PV	1.50	19	Load	0.25	30	Load	0.50
9	WT	1.50	20	Load	0.50	31	MG	2.00
10	Load	0.50	21	MG	4.00	32	PV	1.75
11	PV	1.50	22	WT	2.50	33	Load	0.25

39,40]. Precisely, the looped values referring to the maximum depth are $md \in S_{md} = \{6,7,\ 8,\ 10,\ 12\}$. The analysed features by tree values are $cs \in S_{cs} = \{0.4,0.6,0.8,1\}$. The number of estimators looped are $ne \in S_{ne} = \{500,\ 600,\ 700,\ 800,\ 900\}$. The learning rate is sought in the set $lr \in S_{lr} = \{0.1, 0.01\}$.

For the three considered test sets, the performances of the proposed algorithm are evaluated computing the following quantities: G_C representing the count of the samples for which the model correctly estimates the related class, i.e., $\widehat{C}_{\diagup} = C_{\diagup}$; G_H representing the count of the samples for which the model estimates $\widehat{C}_{\diagup} > C_{\diagup}$; G_L representing the count of the samples for which the model estimates $\widehat{C}_{\diagup} < C_{\diagup}$.

4. Simulations and results

4.1. Algorithm implementation results

For the XGB algorithm created, the best parameters configuration is obtained for $md = 7$, $cs = 0.6$, $ne = 700$, $lr = 0.1$. The outcomes for the best parameters configuration drive to $G_C = 13397, G_H = 1095, G_L =$ 292 on the Test Set 1, and are summarized in Fig. 4(a). In Fig. 4(a) it can be seen that ~90 % of the Test Set 1 samples are correctly classified, i.e., $\widehat{C}_{\diagup} = C_{\diagup}$, for 7.4 % of the test set samples the model predicts $\widehat{C}_{\diagup} > C_{\diagup}$, and for 2 % of the Test Set 1 samples the model predicts $\widehat{C}_{\diagup} < C_{\diagup}$. These results suggest that the model can estimate the exact configuration in ~90 % of cases, thus demonstrating the effectiveness of the algorithm implemented. To deeper analyse the outcomes and to seek possible links among the misclassified samples, the performance referred to each week included in the Test Set 1 is separately computed. An example of the outcomes referred to one week per season over one year extracted from the Test Set 1 is shown in Fig. 4(b). The analysis over each week drive to the following result: the percentage of samples belonging to G_C is always higher than 88.8 %, the percentage of samples belonging to $G_H(G_L)$ reaches, in the worst case, the value of 8.3 % (4.2 %.). For all the weeks, no specific patterns or combinations of the values assumed by the features are identified. Consequently, the outcomes obtained analysing separately each week within the Test Set 1 suggest that the misclassifications cannot be associated with defined combinations of the values assumed by the features and this fact demonstrates that the model is not biased to particular feature characteristics, thus ensuring the generalization abilities to unseen data.

Results of sensitivity analysis performed using Test Set 2 and 3 are shown respectively in Fig. 5 and Fig. 6. Fig. 5(a) demonstrates that, after the application of ± 5 % input data perturbation considered for Test Set 2, the model can correctly estimate the network configuration in 90.8 % of cases.

Similarly, Fig. 6(a) shows that, when input data are perturbed by ± 10 %, the model can still correctly estimate the best network configuration in 89.6 % of cases. These results highlight the low sensitivity of the algorithm to small variations in the input data, underlining the generalization capabilities of XGB models. Similar conclusions can be inferred by examining the seasonal subdivision of the results associated to Test Set 2 and 3, reported in Fig. 5(b) and Fig. 6(b) for the sake of completeness. As far as the computational time is concerned, the training phase of the XGB algorithm is completed in two hours on a medium performance computer. The computational time to calculate to score for a generic sample is equal to 0.198 s, underscoring the computational efficiency of the proposed algorithm. This performance

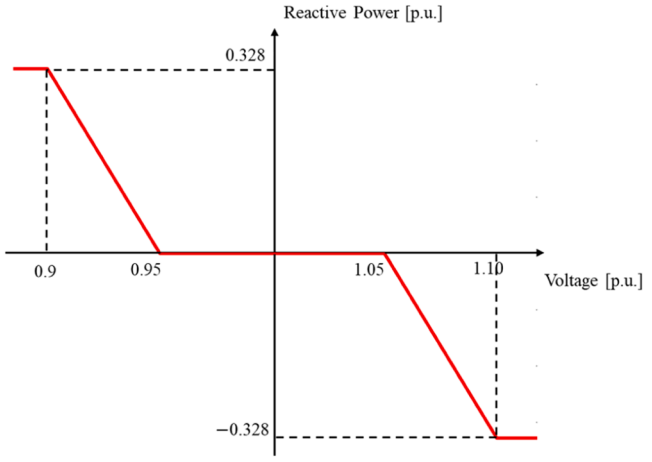

Fig. 3. Voltage vs. Reactive Power curve used to considered RES voltage support.

Table 6
Clusters voltage violation configurations.

Name	Clusters Condition
V_0	No clusters experience under(over)voltage
V_1	One cluster experience under(over)voltage
V_2	Two cluster experience under(over)voltage
V_3	Three cluster experience under(over)voltage
V_4	All clusters experience under(over)voltage

Table 7
Scoring matrix for the considered test case.

Switches status	Clusters Condition				
	V_0	V_1	V_2	V_3	V_4
Radial	40	32	24	16	8
Configuration 1	39	31	23	15	7
Configuration 2	38	30	22	14	6
Configuration 3	37	29	21	13	5
Configuration 4	36	28	20	12	4
Configuration 5	35	27	19	11	3
Configuration 6	34	26	18	10	2
Configuration 7	33	25	17	9	1

Table 8
Samples extracted from the training portion of the Output Dataset.

Features																		Target
PV_1	PV_2	PV_3	…	WT_1	WT_2	WT_3	…	$Load_1$	$Load_2$	$Load_3$	…	MG_1	MG_2	MG_3	$INT_{13–33}$	$INT_{18–25}$	$INT_{5–22}$	Class
0.28	0.38	0.49	…	0.83	1.723	0.22	…	0.15	0.73	0.31	…	0.27	0.47	0.2	0	0	0	C_1
0.28	0.38	0.49	…	0.83	1.723	0.22	…	0.15	0.73	0.31	…	0.27	0.47	0.2	1	0	0	C_2

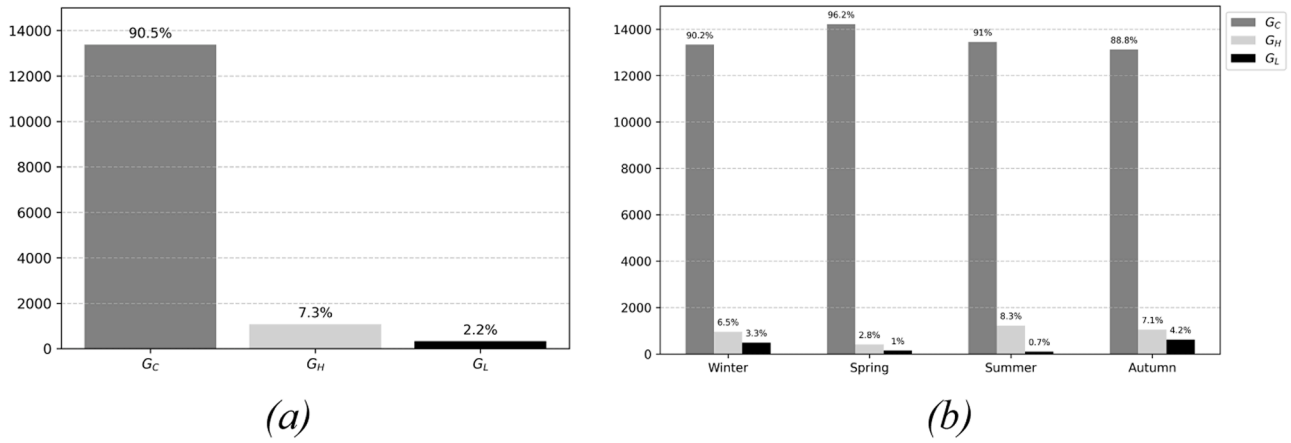

Fig. 4. Percentage values of G_C, G_H and G_L, referred to the samples for Test Set 1 (a) aggregated data, (b) split per season.

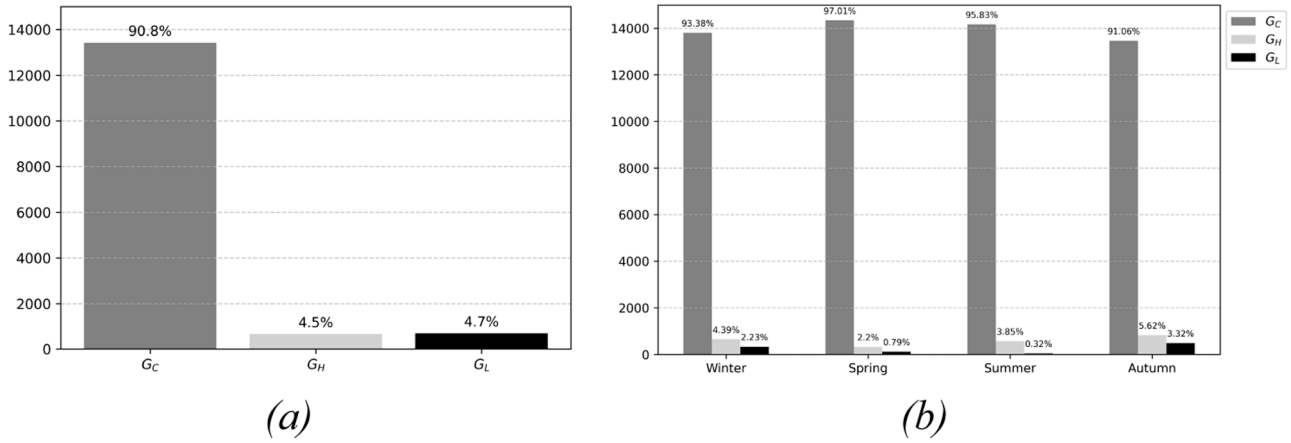

Fig. 5. Percentage values of G_C, G_H and G_L, referred to the samples for Test Set 2 (a) aggregated data, (b) split per season.

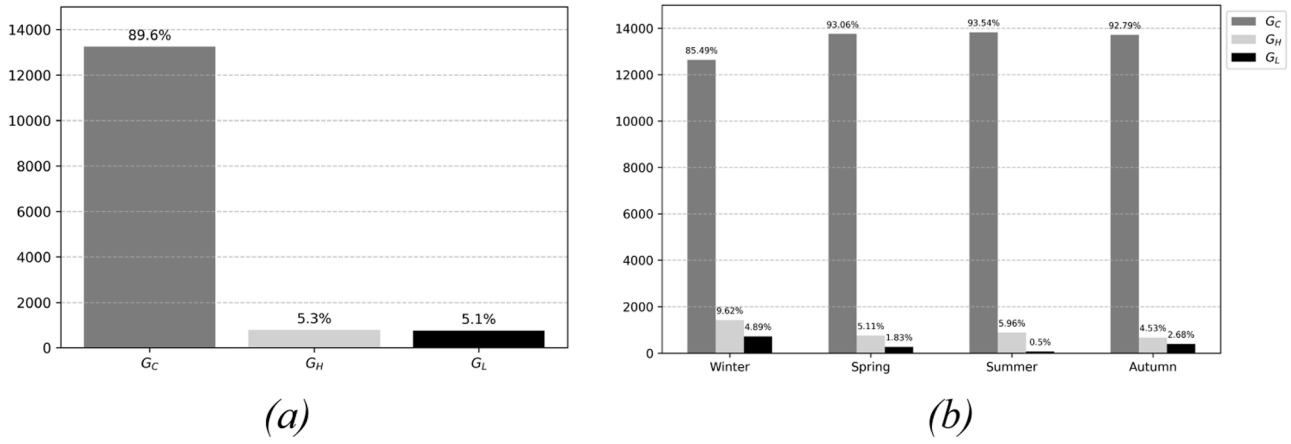

Fig. 6. Percentage values of G_C, G_H and G_L, referred to the samples for Test Set 3 (a) aggregated data, (b) split per season.

marks an improvement of 30 % with respect to the execution time reported in [15] for a decision tree based algorithm and shows better performance than the deep learning-based approaches in [27], reducing of 40 % the computational time.

4.2. SDACA tool application results

The SDACA utilization of the results provided by the algorithm is done with reference to the hours corresponding to the considered test sets. Since the samples are eight time the actual working points of the Power Profile Dataset, the validation shall be done with reference to 1,848 hours of the Power Profile Dataset for each test set. The validation of the SDACA tool is performed using DigSILENT PowerFactory® for power flow calculations, comparing the expected outcome of the SDACA optimal configuration with the radial configuration, which is typically used to operate the distribution network. Firstly, to highlight the detailed implementation of the SDACA, results are shown for 4 hours extracted from Test Set 1; more specifically, one for each season, detailed input values of selected hours are reported in the attached dataset[1]. The SDACA evaluates each configuration using the XGB algorithm and selects the one with the highest score. For the sake of clarity, the upper panels of Fig. 7 report the nodes voltage calculated by exact load flow calculation for the considered week while the lower panels plot the configuration selected the proposed SDACA tool to reconfigure the grid and solve voltage problems. As an example, for the spring hour, the SDACA tool identifies Configuration 3 as the optimal one, as it achieves the highest score among the eight configurations. Therefore, starting from the radial configuration of the distribution network, the SCADA requires to close only switch $INT_{5\text{-}22}$ to minimize both the number of reclosers and the voltage violations in the spring hour. Similarly, Configuration 4 represents again the optimal configuration for the summer hour, while Configuration 2 is optimal for the autumn hour, and the radial configuration is preferred for the winter hour. It is worth recalling that the optimal configuration is determined by the SDACA based on the scores assigned by the XGB algorithm and corresponds to the configuration with the highest score, as shown in Table 9, where scores has been calculated on the basis of load flow calculations for validation.

After showing detailed implementation for the selected hours, assessment of SDACA performance for the considered test sets are provided. Fig. 8 shows the number of violations for each node in the SDACA configuration compared to the radial configuration for the 1,848 h of Test Set 1.

In Test Set 1, operating the system in the radial configuration, 10,385 bus voltage violations are found (sum of all red column in Fig. 8). As one can notice, the SDACA has a beneficial effect on voltage violations since the SDACA proposed reconfiguration reduces to overall voltage violations to 3,781 corresponding to a 63.59 % reduction of the overall voltage violations of the radial configuration.

Moreover, it is worth pointing out that, for the considered test case, network feeder reconfiguration is not supposed to be able to solve all voltage violations. In fact, by post processing the Test Set 1 with a brute force approach, it was possible pointing out that, the minimum number of violations if the best configuration is always implemented is equal to 3,707 violations. This confirms the effectiveness of the implemented SDACA due to the marginal discrepancy with the maximum possible impact of grid reconfiguration for the considered test set with a very fast and performing data driven algorithm. A similar analysis is performed considering Test Set 2 and Test Set 3. Overall voltage violation for Test Set 2 and Test Set 3 if radial configuration is considered are equal to 10,397 and 10,384 respectively. SDACA application for these two additional test sets can reduce overall voltage violations to 3,708 for Test Set 2 and 3724 for Test Set 3, corresponding to a violation reduction of a 64.34 % and 64.24 %. As previously mentioned, the minimum voltage violations for Test Set 2 and Test Set 3 if the optimal configuration would be always selected are equal to 3,702 and 3,701 respectively, confirming the highly relevant results of the proposed algorithm. Graphical comparisons of voltage violations obtained by the application

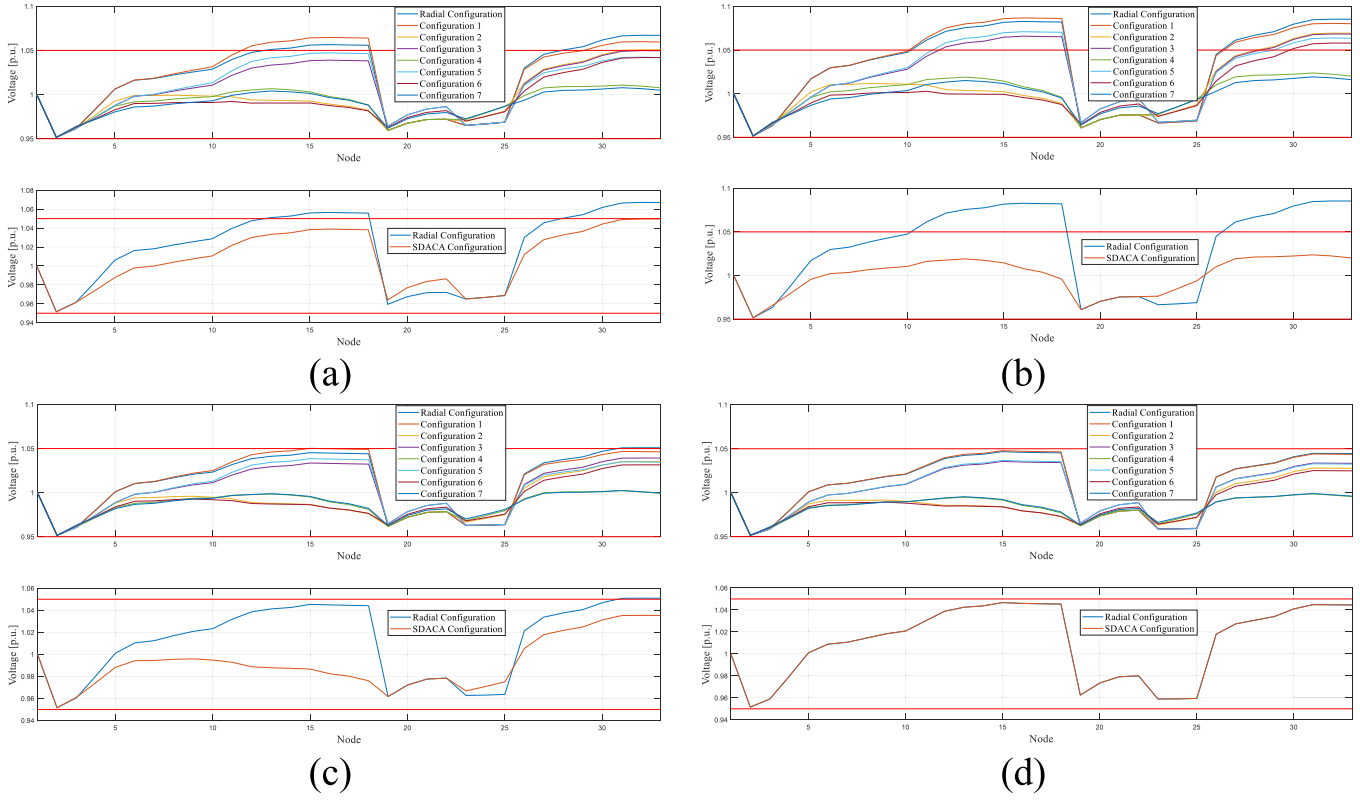

Fig. 7. Voltage values in all network configurations and SDACA response for the spring (a), summer (b), autumn (c) and winter (d) hour.

Table 9
Configuration scoring for the 4 h detailed for validation.

Configuration	Spring	Summer	Autumn	Winter
Radial	24	24	32	40
Configuration 1	23	23	31	39
Configuration 2	30	30	38	38
Configuration 3	37	21	37	37
Configuration 4	36	36	36	36
Configuration 5	35	19	35	35
Configuration 6	34	26	34	34
Configuration 7	33	33	33	33

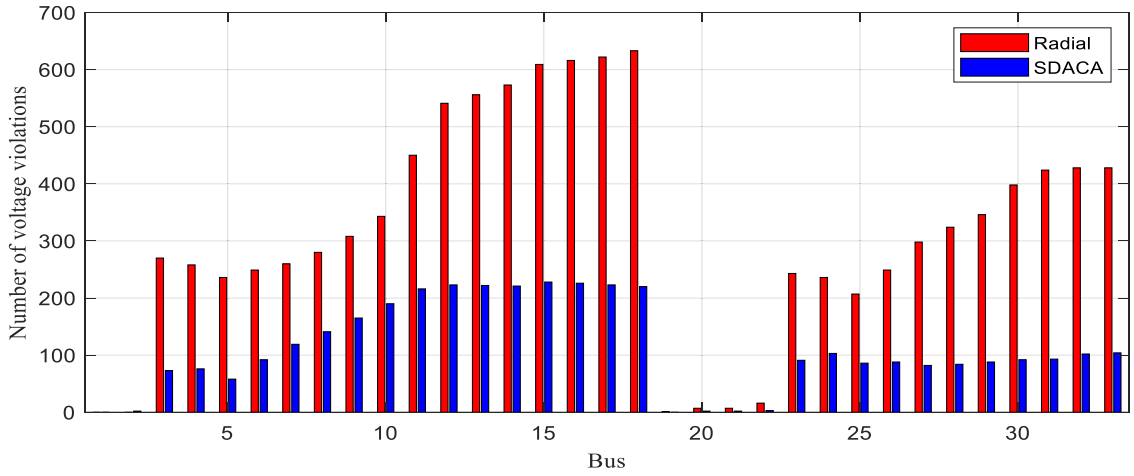

Fig. 8. Bus voltage violations: SDACA configuration vs. radial for Test Set 1.

of the proposed SDACA tool against radial configuration are reported in Fig. 9 and Fig. 10 for Test Set 2 and Test Set 3.

A summary of effectiveness of the SDACA tool in the considered test sets is reported in Table 10. As one can notice results point out a relevant effectiveness of the proposed SDACA tool in solving voltage violation, obtaining an impact sensibly close to the maximum affordable impact that network feeder reconfiguration can provide.

As a final remark, one can notice that the accuracy of the proposed SDACA tool in finding the most effective solution is very high. This is related to the fact that, in the case of XGB marginal misclassification of the configuration scoring, if the voltage violation condition is the same as the optimal configuration, maximum impact on voltage violation is achieved anyway, probably not with the minimum number of reclosure, but this is a negligible drawback in the light of the capabilities of the proposed approach.

5. Conclusion

This paper proposed a pattern recognition tool to support distribution system operators in managing network reconfiguration with the

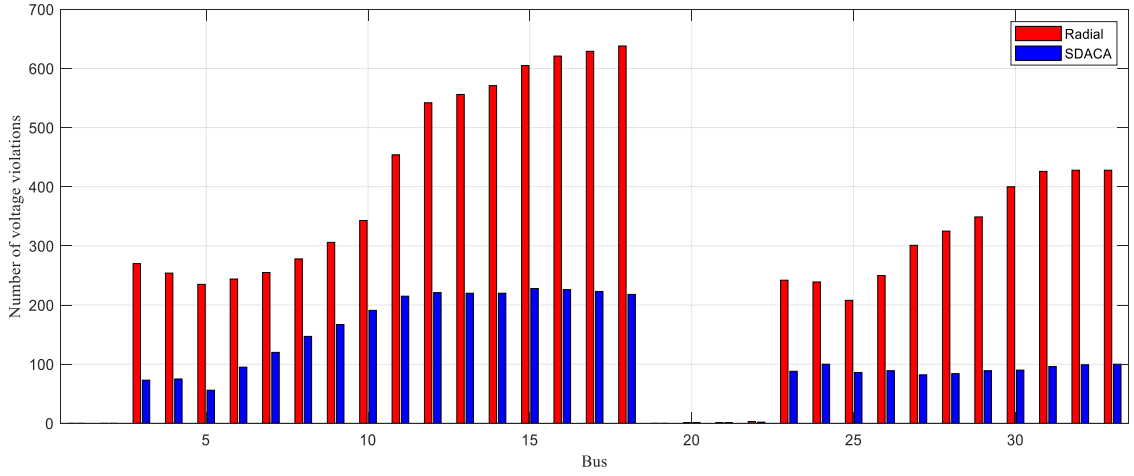

Fig. 9. Bus voltage violations: SDACA configuration vs. radial for Test Set 2.

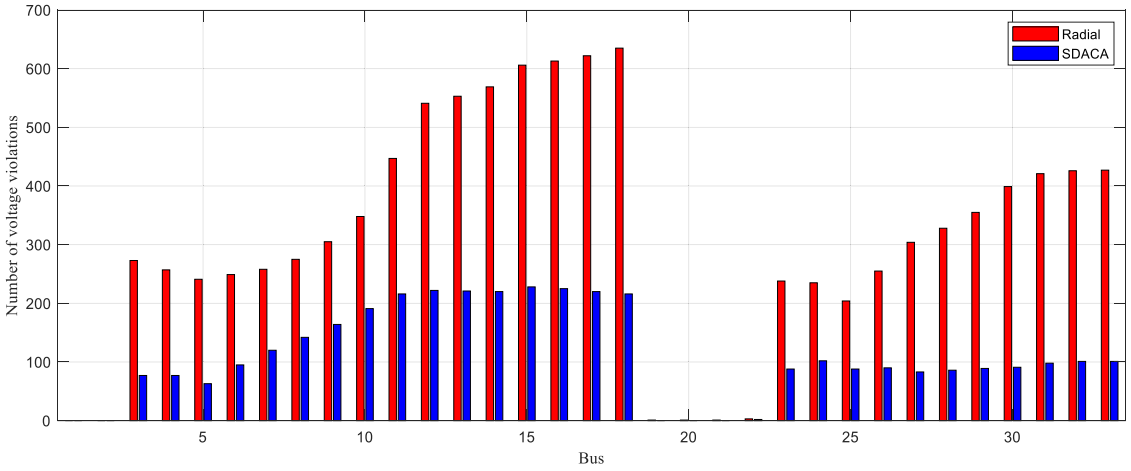

Fig. 10. Bus voltage violations: SDACA configuration vs. radial for Test Set 3.

Table 10
Metrics for evaluating the performance of the SDACA.

Dataset	Violations Radial	Violations SDACA Config.	Violation reduction	Minimum violations with optimal config.	SDACA accuracy on voltage violations
Test Set 1	10,385	3,781	63.59 %	3,707	98.00 %
Test Set 2	10397	3,708	64.34 %	3,702	99.83 %
Test Set 3	10,384	3,724	64.24 %	3,701	99.38 %

aim of limiting steady-state violation introduced by relevant share of renewable energy sources in distribution power systems. To this goal, a pattern recognition algorithm was implemented to estimate the optimal network topology to minimize overvoltage and undervoltage issues at the network nodes, as well as the number of reclosures within the originally radial network. The smart distribution area control architecture leverages the extreme gradient boosting algorithm to evaluate and assign scores to the possible network configurations, selecting the configuration with the highest score. The tool was implemented and tested on the IEEE 33-bus system and compared in terms of voltage violations with the commonly adopted radial configuration. Three tests to include a sensitivity analysis of the performance of the tool when input data are perturbed were also implemented. The outcomes of the tests demonstrated that the algorithm allows to perform a fast-training procedure and to estimate the reconfiguration of all alternative network topologies in a short time intervals. The seasonal analysis highlighted the operational approach of the tool and its effectiveness in identifying the optimal configuration of the distribution network. The implementation of the SDACA tool on the IEEE 33-bus distribution network demonstrated significant improvements in performance compared to the traditional radial configuration. Results achieved highlighted that the proposed approach allows solving around 64 % of voltages violations and can achieve an accuracy in voltage reduction compared to the maximum possible impact of feeder reconfiguration actions over 98 % for all the considered test sets. Computational time experienced on a medium performance computer underlines the capabilities of the tool for realistic applications and possible real-time application of the proposed methodology even for more extended grids and improved. However, it is highlighted that the effectiveness of the approach and the classification error rate are influenced by the representativeness of the training dataset. This approach requires extensive and representative grid operation data to effectively train the algorithm. However, since the tool is primarily intended for use by the DSO, who typically has access to substantial historical data and forecasts regarding the network's evolution, this limitation is less pronounced in the specific context for which the SDACA has been designed. Under this perspective, future work will be dedicated to the enhancement of the algorithm performance and of the tool, extending beyond the mitigation of overvoltage and undervoltage issues to also encompass transformer and line overloads, as well as line losses, thereby ensuring a more effective and comprehensive approach to network management.

CRediT authorship contribution statement

Andrea Bonfiglio: Writing – review & editing, Supervision, Methodology, Funding acquisition, Data curation. **Alice La Fata:** Writing – original draft, Validation, Methodology, Investigation, Conceptualization. **Manuela Minetti:** Writing – original draft, Validation, Methodology, Investigation, Data curation.

Declaration of competing interest

The authors declare that they have no known competing financial interests or personal relationships that could have appeared to influence the work reported in this paper.

Acknowledgement

Research founded by European Union NextGEneration EU

Data availability

Data attached as supplementary material

References

[1] A.M. Helmi, R. Carli, M. Dotoli, H.S. Ramadan, Efficient and sustainable reconfiguration of distribution networks via metaheuristic optimization, IEEE Trans. Autom. Sci. Eng. 19 (1) (2021) 82–98.
[2] W. Huang, W. Zheng, D.J. Hill, Distribution network reconfiguration for short-term voltage stability enhancement: an efficient deep learning approach, IEEE Trans. Smart. Grid. 12 (6) (2021) 5385–5395.
[3] K. Mardanimajd, S. Karimi, A. Anvari-Moghaddam, Voltage stability improvement in distribution networks by using soft open points, Int. J. Electr. Power Energy Syst. 155 (2024) 109582.
[4] A. Bonfiglio, M. Fresia, M. Minetti, R. Procopio, A. Rosini, G. Lisciandrello, L. Orrù, Inertia requirements assessment for the Italian transmission network in the future network scenario, IEEE (2023) 1–5.
[5] X. Hu, Z.W. Liu, G. Wen, X. Yu, C. Liu, Voltage control for distribution networks via coordinated regulation of active and reactive power of DGs, IEEE Trans. Smart. Grid. 11 (5) (2020) 4017–4031.

[6] Z. Tang, D.J. Hill, T. Liu, Distributed coordinated reactive power control for voltage regulation in distribution networks, IEEE Trans. Smart. Grid. 12 (1) (2020) 312–323.
[7] A. Bonfiglio, S. Bruno, M. Martino, M. Minetti, R. Procopio, A. Velini, Renewable energy communities virtual islanding: a novel service for smart distribution networks, IEEE (2024) 1–8.
[8] A. Rosini, A. Bonfiglio, D. Mestriner, M. Minetti, S. Bracco, A simplified study for reactive power management in autonomous microgrids, WSEAS Trans. Power Syst. 14 (2019) 107–112.
[9] A. Serrano-Fontova, M. Azab, Development and performance analysis of a multi-functional algorithm for AC microgrids: simultaneous power sharing, voltage support and islanding detection, Int. J. Electr. Power Energy Syst. 135 (2022) 107341.
[10] X. Zhang, Y. Yang, H. Zhao, Y. Luo, X. Xu, Two-stage optimal scheduling of an islanded microgrid considering uncertainties of renewable energy, Int. J. Electr. Power Energy Syst. 162 (2024) 110324.
[11] D.S. Rani, N. Subrahmanyam, M. Sydulu, Multi-objective invasive weed optimization–an application to optimal network reconfiguration in radial distribution systems, Int. J. Electr. Power Energy Syst. 73 (2015) 932–942.
[12] T. Niknam, A.K. Fard, A. Seifi, Distribution feeder reconfiguration considering fuel cell/wind/photovoltaic power plants, Renew. Energy 37 (1) (2012) 213–225.
[13] Y. Qu, C.C. Liu, J. Xu, Y. Sun, S. Liao, D. Ke, A global optimum flow pattern for feeder reconfiguration to minimize power losses of unbalanced distribution systems, Int. J. Electr. Power Energy Syst. 131 (2021) 107071.
[14] R.A. Jabr, R. Singh, B.C. Pal, Minimum loss network reconfiguration using mixed-integer convex programming, IEEE Trans. Power. Syst. 27 (2) (2012) 1106–1115.
[15] D. Sarkar, S.K. Gunturi, Machine learning enabled steady-state security predictor as deployed for distribution feeder reconfiguration, J. Electr. Eng. Technol. 16 (2021) 1197–1206.
[16] F.V. Gomes, S. Carneiro, J.L.R. Pereira, M.P. Vinagre, P.A.N. Garcia, L.R. De Araujo, A new distribution system reconfiguration approach using optimum power flow and sensitivity analysis for loss reduction, IEEE Trans. Power. Syst. 21 (4) (2006) 1616–1623.
[17] H.P. Schmidt, N. Ida, N. Kagan, J.C Guaraldo, Fast reconfiguration of distribution systems considering loss minimization, IEEE Trans. Power. Syst. 20 (3) (2005) 1311–1319.
[18] M.R. Dorostkar-Ghamsari, M. Fotuhi-Firuzabad, M. Lehtonen, A. Safdarian, Value of distribution network reconfiguration in presence of renewable energy resources, IEEE Trans. Power. Syst. 31 (3) (2015) 1879–1888.
[19] H.M. Ahmed, M.M. Salama, Energy management of AC–DC hybrid distribution systems considering network reconfiguration, IEEE Trans. Power. Syst. 34 (6) (2019) 4583–4594.
[20] A. La Fata, M. Brignone, R. Procopio, S. Bracco, F. Delfino, R. Barilli, M. Ravasi, F. Zanellini, M. Petronijevic, A simulator for long term planning and real time scheduling of polygenerative microgrids, in: *2023 IEEE Belgrade PowerTech*, IEEE, 2023, pp. 1–6.
[21] Y. Gao, W. Wang, J. Shi, N. Yu, Batch-constrained reinforcement learning for dynamic distribution network reconfiguration, IEEE Trans. Smart. Grid. 11 (6) (2020) 5357–5369.
[22] R. Baldick, F.F. Wu, Approximation formulas for the distribution system: the loss function and voltage dependence, IEEE Trans. Power Deliv. 6 (1) (1991) 252–259.
[23] W. Guan, Y. Tan, H. Zhang, J. Song, Distribution system feeder reconfiguration considering different model of DG sources, Int. J. Electr. Power Energy Syst. 68 (2015) 210–221.
[24] H. Haghighat, B. Zeng, Distribution system reconfiguration under uncertain load and renewable generation, IEEE Trans. Power. Syst. 31 (4) (2015) 2666–2675.
[25] S. Essallah, A. Khedher, Optimization of distribution system operation by network reconfiguration and DG integration using MPSO algorithm, Renew. Energy Focus 34 (2020) 37–46.
[26] A. Mishra, M. Tripathy, P. Ray, A survey on different techniques for distribution network reconfiguration, J. Eng. Res. 12 (1) (2024) 173–181.
[27] H. Gao, R. Wang, S. He, L. Wang, J. Liu, Z. Chen, A cloud-edge collaboration solution for distribution network reconfiguration using multi-agent deep reinforcement learning, IEEE Trans. Power. Syst. 39 (2) (2023) 3867–3879.
[28] S.H. Oh, Y.T. Yoon, S.W. Kim, Online reconfiguration scheme of self-sufficient distribution network based on a reinforcement learning approach, Appl. Energy 280 (2020) 115900.
[29] H. Kim, Y. Ko, K.H. Jung, Artificial neural-network based feeder reconfiguration for loss reduction in distribution systems, IEEE Trans. Power Deliv. 8 (3) (1993) 1356–1366.
[30] M. Kashem, G. Jasmon, A. Mohamed, M. Moghavvemi, Artificial neural network approach to network reconfiguration for loss minimization in distribution networks, Int. J. Electr. Power Energy Syst. 20 (4) (1998) 247–258.
[31] A. La Fata, M.A. Amin, M. Invernizzi, R. Procopio, Structurally tuned LSTM networks to nowcast photovoltaic power production. 2024 IEEE International Conference on Environment and Electrical Engineering and 2024 IEEE Industrial and Commercial Power Systems Europe (EEEIC/I&CPS Europe), 2024, pp. 1–6.
[32] S.M. Lundberg, G. Erion, H. Chen, A. DeGrave, J.M. Prutkin, B. Nair, R. Katz, J. Himmelfarb, N. Bansal, S.I. Lee, From local explanations to global understanding with explainable AI for trees, Nat. Mach. Intell. 2 (1) (2020) 56–67.
[33] N. Krishnan, K.R. Kumar, Solar radiation forecasting using gradient boosting based ensemble learning model for various climatic zones, Sustain. Energy Grids Netw. 38 (2024) 101312.
[34] L.F. Grisales-Noreña, J.C. Morales-Duran, S. Velez-Garcia, O.D. Montoya, W. Gil-González, Power flow methods used in AC distribution networks: an analysis of convergence and processing times in radial and meshed grid configurations, Results. Eng. 17 (2023) 100915.
[35] A. Sharma, R. Tiwari, Anomaly detection in smart grid using optimized extreme gradient boosting with SCADA system, Electr. Power Syst. Res. 235 (2024) 110876.
[36] M.A. Amin, A. La Fata, R. Procopio, M. Invernizzi, M. Petronijevic, I.R Mitic, Photovoltaic power nowcasting using decision-trees based algorithms and neural networks, in: 2024 11th International Conference on Electrical, Electronic and Computing Engineering (IcETRAN), 2024, pp. 1–6.
[37] T. Chen, C. Guestrin. Xgboost: a scalable tree boosting system, Proceedings of the 22nd acm sigkdd international conference on knowledge discovery and data mining, 2016, pp. 785–794.
[38] Murphy K.P. Probabilistic Machine Learning: an Introduction. MIT Press; 2022.
[39] Y. Wang, S. Sun, X. Chen, X. Zeng, Y. Kong, J. Chen, Y. Guo, T. Wang, Short-term load forecasting of industrial customers based on SVMD and XGBoost, Int. J. Electr. Power Energy Syst. 129 (2021) 106830.
[40] R.K. Agrawal, F. Muchahary, M.M. Tripathi, Ensemble of relevance vector machines and boosted trees for electricity price forecasting, Appl. Energy 250 (2019) 540–548.
[41] Comitato Elettrotecnico Italiano. CEI 0-16 - reference technical rules for the connection of active and passive consumers to the HV and MV electrical networks.
[42] N.L. Dehghani, A. Shafieezadeh, Multi-stage resilience management of smart power distribution systems: a stochastic robust optimization model, IEEE Trans. Smart. Grid. 13 (5) (2022) 3452–3467.